Vol. 29 (1998) *ACTA PHYSICA POLONICA B* No 11

CHIRAL DYNAMICS IN DENSE MATTER: IN-MEDIUM MESON SPECTRA*

F. Klingl and W. Weise

Physik-Department, Technische Universität München
85747 Garching, Germany

(Received June 22, 1998)

We summarize recent developments related to meson spectra in a dense nuclear medium. Our primary emphasis is on vector meson mass spectra in matter and their role as possible indicators of a tendency toward restoration of spontaneously broken chiral symmetry.

PACS numbers: 24.85.+p, 12.38.–t

1. Introduction

QCD with massless u-, d-, and s-quarks has a chiral $\mathrm{SU(3)_L}\times\mathrm{SU(3)_R}$ symmetry. As a consequence of strong QCD forces, this symmetry is spontaneously broken. It is also explicitly broken by the quark masses. This symmetry breaking pattern is clearly manifest in the low energy hadron spectrum, with the octet of light pseudoscalar mesons representing the Goldstone bosons of the spontaneously broken symmetry. No parity doublets are observed. For example, the masses of the ($J^\pi = 1^-$) vector mesons are systematically lower than those of their chiral partners, the ($J^\pi = 1^+$) axial vector mesons.

Spontaneously broken chiral symmetry is expected to be restored at high temperatures and high baryon densities. At this point vector and axial vector modes become degenerate, and one expects that in-medium vector meson spectra should show traces of this tendency. One of the issues of chiral dynamics in dense matter is then to explore the driving mechanisms for chiral restoration. The framework for our discussion is an effective Lagrangian, based on chiral $\mathrm{SU(3)_L}\times\mathrm{SU(3)_R}$ symmetry, which incorporates the interactions of the Goldstone bosons (pions, kaons) with the octets of baryons and vector mesons [1].

* Presented at the Meson'98 and Conference on the Structure of Meson, Baryon and Nuclei, Cracow, Poland, May 26–June 2, 1998.

2. Pions and kaons in matter: brief summary

Before focusing on vector meson spectra in a dense nuclear medium, let us give a brief summary on recent progress in our understanding of the in-medium behaviour of pions and kaons.

Chiral dynamics predicts the leading s-wave interactions of pions in nuclear matter. For example, a π^- in a typical heavy nucleus with a substantial neutron excess, like Pb, should experience a moderately repulsive central potential of about 20–25 MeV [2]. This has been beautifully confirmed by the recent observation of deeply bound pionic states using the $^{208}\mathrm{Pb}(d, ^3\mathrm{He})(\pi^- \oplus ^{207}\mathrm{Pb})$ reaction at GSI [3].

Chiral SU(3) dynamics also predicts a characteristic splitting of the K^+ and K^- masses in nuclear matter. The K^+ is expected to experience weak repulsion, whereas the K^- feels a strongly attractive potential of order -100 MeV at normal nuclear matter density, $\varrho = \varrho_0 = 0.17\ \mathrm{fm}^{-3}$. While various approaches differ in their quantitative details [4, 5], a consistent qualitative picture has emerged. This picture is supported by the recently measured subthreshold K^-/K^+ production ratios at GSI/SIS [6].

3. Vector meson spectra in dense matter

Let us now turn to the in-medium behaviour of ρ, ω and ϕ mesons. The basic quantity to start with is the current–current correlation function

$$\Pi_{\mu\nu}(\omega, \vec{q}) = i \int_{-\infty}^{+\infty} dt \int d^3x\, \mathrm{e}^{i\omega t - i\vec{q}\cdot\vec{x}} \langle \mathcal{T} j_\mu(\vec{x}, t) j_\nu(0) \rangle, \tag{1}$$

where j_μ is the electromagnetic current and $\mathcal{T}$ denotes time-ordering. At temperature $T = 0$, the expectation value in Eq. (1) is taken in the ground state of nuclear matter at density ϱ. The imaginary part of $\Pi_{\mu\nu}$ determines the spectrum of vector meson excitations in matter. At finite temperature, this spectrum can be "seen" by detecting the e^+e^- pairs produced in high-energy heavy-ion collisions. The ongoing CERES and forthcoming HADES experiments are aimed at the question whether in-medium spectra differ markedly from the corresponding vacuum spectra observed in the process $e^+e^- \to$ hadrons.

We proceed as follows: Using an effective Lagrangian which combines chiral dynamics with the vector meson dominance of the electromagnetic current, we specify a Lorentz frame in which nuclear matter as a whole is at rest and first study vector meson spectral distributions at $\vec{q} = 0$ as a function of energy ω. In this case only the transverse components of the correlation tensor (1) survives with

$$\Pi_{00} = \Pi_{0i} = \Pi_{j0} = 0 \quad \text{and} \quad \Pi_{ij}(\omega, \vec{q} = 0; \varrho) = -\delta_{ij}\Pi(\omega, \vec{q} = 0; \varrho)\,.$$

This specifies the reduced scalar correlation function Π. It involves the vector meson self-energies Π_V(with $V = \rho, \omega, \phi$) to all orders. At low density, $\Pi_V = \Pi_V(\text{vac}) - \varrho T_{VN}$, where the vacuum quantity $\Pi_V(\text{vac})$ is

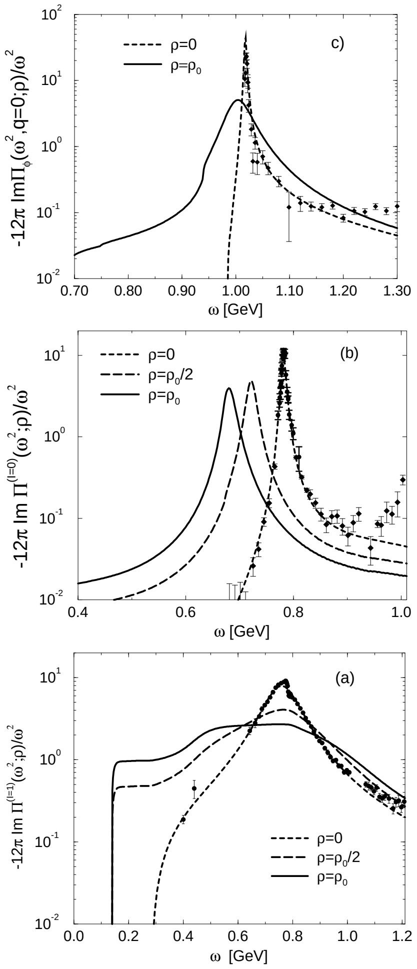

Fig. 1. Spectral distributions in the vector meson channels of the current–current correlation function [7, 8]. The dashed lines show the vacuum spectra in the ρ, ω and ϕ channels normalized such that they can be compared directly with the corresponding $e^+e^- \to$ hadrons data. The long dashed and solid lines show the calculated spectral functions in nuclear matter at densities $\varrho_0/2$ and $\varrho_0 = 0.17\text{fm}^{-3}$, as discussed in Section 3.

known from $e^+e^- \to$ hadrons. The primary problem is now to calculate the T-matrix describing the interactions of vector mesons with nucleons. Details of these calculations are explained in [7, 8].

The results are summarized in Fig. 1. We observe important differences between the various channels. The ρ meson mass is expected to decrease only slightly while the width increases very strongly. This causes the spectral strength to shift downwards and broaden substantially. We also see strong threshold contributions starting at the pion mass. The ρ meson evidently dissolves in nuclear matter; it does not survive as a "good" quasi-particle. On the other hand the mass of the ω meson decreases significantly. Its width also increases but not as strongly as for the ρ meson, so it can still be regarded as a good quasi-particle in matter. For the ϕ meson there is almost no change in the peak position while the width increases.

As demonstrated in [7], the calculated ρ, ω and ϕ spectra are perfectly consistent with in-medium QCD sum rules. There are, of course, uncertainties on both sides of the sum rule analysis. On one side, the calculated spectra have some model dependence related to the vaguely known high-energy behaviour of the vector meson-nucleon amplitudes, and to unknown possible contact terms in the basic interactions. On the other side, in the operator product expansion part of the QCD sum rule, uncertainties exist as to the factorization of four-quark condensates at finite baryon density. In view of this, in-medium QCD sum rules do not have predictive power, but they are useful as a consistency test for calculated mass spectra.

4. Dilepton spectra

In a simple thermal model the dilepton production rates in high-energy heavy-ion collisions are determined by

$$\frac{dR}{d^4x\,d^4q} = \frac{\alpha^2}{\pi^3 q^2} |\mathrm{Im}\,\Pi(q;\varrho,T)| f_{\mathrm{B}}(q_0,T)\,, \tag{2}$$

with $\alpha = e^2/4\pi \simeq 1/137$ and $\Pi = g_{\mu\nu}\Pi^{\mu\nu}/3$. We denote the four-momentum of the dilepton pair by $q = (q_0, \vec{q})$. The space-time volume element which radiates the dilepton pair is d^4x. Apart from the Boltzmann factor $f_{\mathrm{B}} = [\exp(q_0/T) - 1]^{-1}$, the imaginary part of the current–current correlation function completely determines the dilepton yield in this picture which we will use here to outline the primary effects.

We can now compare our results for $\mathrm{Im}\,\Pi$ with the dilepton data measured by CERES [9]. The produced dileptons in this experiment carry three-momenta $|\vec{q}|$ of the same order as their invariant mass, so we have to include p-wave interactions of the ρ meson with nucleons as in [10]. We incorporate the relevant N^* and Δ resonances (the $\Delta(1232)$, $N^*(1720)$ and $\Delta^*(1905)$) in the calculation. For the ωN and ϕN systems no such resonances are known. The resulting momentum dependent amplitudes $T_{VN}(\omega, \vec{q})$ are then included in Eq. (2).

The explicit temperature dependence of $\mathrm{Im}\,\Pi$ is generally found to be quite weak, so that we can use $\mathrm{Im}\,\Pi(q; \varrho, T = 0)$ as a good first approximation and leave the temperature dependence entirely to the Boltzmann factor f_{B}.

The differential production rate of the e^+e^- pairs with respect to rapidity η and invariant mass m is then determined as follows:

$$\frac{d^2N_{e^+e^-}}{d\eta\, dm} = \int_0^{t_f} dt V(t) \int d^3q\, \frac{m}{q_o} \cdot \frac{dR(q; \varrho(t), T(t))}{d^4x\, d^4q} A(q)\,. \tag{3}$$

The integrals are taken over the time evolution of the expanding fireball from its formation at $t = 0$ until the freeze-out time t_f, and the acceptance $A(q)$ of the detector. The density profile $\varrho(t)$ and the temperature profile $T(t)$ for the evolving fireball are adjusted to agree with more involved transport calculations [11]. We use $T(t) = (T_i - T_\infty)\mathrm{e}^{-t/\tau_1} + T_\infty$ with $T_i = 170$ MeV, $T_\infty = 110$ MeV, $\tau_1 = 8$ fm and $\varrho(t) = \varrho_i \exp(-t/\tau_2)$ with $\varrho_i = 2.5\varrho_0, \tau_2 = 5$ fm. An overall normalization factor is set by the result of transport calculations using the vacuum vector meson spectra, in the absence of in-medium modifications. This normalization factor presumably accounts, among other things, for non-equilibrium dynamics in the transport equations which is ignored in the crude thermal approach.

Despite its extreme simplicity, the thermal model together with the calculated in-medium spectral distributions reproduces the CERES data quite well, as shown in Fig. 2(a). Qualitatively similar results have been found in [10]. This figure also shows that the resonant p-wave ρN dynamics at $\vec{q} \neq 0$ has only a moderate effect. The primary feature is the strong broadening of the in-medium ρ meson spectrum which shifts spectral strength to low e^+e^- invariant masses. The ω and ϕ peaks, not seen by CERES because of limited energy resolution, remain essentially at their unperturbed positions since they are formed in the final phase of the expansion. By that time the baryon density has already decreased to a fraction of normal nuclear matter density.

One should note that the apparent "hill" structure in the data below the free ρ resonance and above 0.2 GeV is entirely due to the CERES detector acceptance $A(q)$. Setting $A(q) \equiv 1$ produces an equivalent, structureless spectrum which is reminiscent of a simple thermal spectrum with a characteristic temperature $T = 170$ MeV.

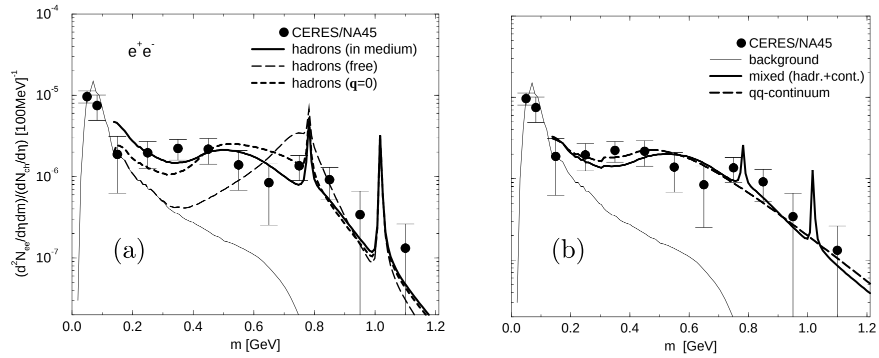

Fig. 2. Comparison of the dilepton rates from sulfur on gold collisions measured by the CERES collaboration; — (a) hadronic scenario with (solid) and without (dashed) medium modifications. The short-dashed line shows the in-medium result when finite $\vec{q}$ effects are neglected. — (b) Mixed scenario with free $q\bar{q}$ pairs at $T > T_c = 150$ MeV and hadrons at $T < T_c$ (solid). The dashed curve shows the limiting case of a purely uncorrelated $q\bar{q}$ spectrum.

At this point one might raise doubts whether a hadronic scenario is at all appropriate. If the initial temperature of the fireball is indeed that large, the system may have already passed through a phase (at critical temperature $T_c \simeq 150$ MeV) in which chiral symmetry is (approximately) restored. In this phase with $T_i > T > T_c$ the sources which radiate e^+e^- pairs should be almost free quark-antiquark pairs rather than mesons. We have therefore tried a mixed scenario which starts out, at $T_i = 170$ MeV, with a free $q\bar{q}$ continuum, $(-12\pi/q^2)\mathrm{Im}\Pi(q^2) = 5/3$ for $4m_{u,d}^2 \leq q^2 \leq m_s^2$ and equal to 2 above the strange quark threshold, with current quark masses $m_{u,d} \simeq 10$ MeV and $m_s \simeq 150$ MeV. When the temperature reaches $T_c \simeq 150$ MeV, the system is assumed to cross over to the hadronic phase, with $\mathrm{Im}\Pi$ determined as before. The result is shown in Fig. 2(b). At the present level of data statistics, it cannot be distinguished from the purely hadronic scenario, Fig. 2(a), except that the mixed scenario produces more strength at masses above the ϕ meson. Notably, a completely flat free $q\bar{q}$ continuum corresponding to a spectrum $(-12\pi/q^2)\mathrm{Im}\Pi = \text{const.}$, would also be in accordance with the data.

5. Nuclear bound states of ω mesons

Given the obvious uncertainties encountered in ultra-relativistic heavy-ion collisions, it is certainly useful to explore in-medium effects under less extreme, better controlled conditions. The ω meson is clearly an interesting candidate. The driving ωN interactions based on the chiral effective Lagrangian (with inclusion of anomalies) suggest strong in-medium attraction, corresponding to a mass shift of about -100 MeV at normal nuclear matter density.

In the local density approximation, the ω meson self-energy can be translated into a complex, energy dependent potential

$$\mathcal{U}\,(E,\vec{r}) = \frac{1}{2E}\left[\Pi_{\rm vac}(E) - T_{\omega N}(E)\rho(\vec{r})\right]. \tag{4}$$

Terms involving $\vec{\nabla}\rho(\vec{r})\cdot\vec{\nabla}$ are expected to be less important. Here $\Pi_{\rm vac}$ is the self-energy in free space which incorporates the $\omega \to 3\pi$ decay. The ωN amplitude $T_{\omega N}(E)$ is strongly energy dependent. Its real part is positive for $E > 0.4$ GeV and turns negative at lower energies. Its imaginary part represents the $\omega N \to \pi N, \pi\pi N$ *etc.* reaction channels. Unlike the ρ meson case, the in-medium decay width of the ω meson turns out not to be overwhelming, given that the $\omega \to 3\pi$ width in free space is only about 7.5 MeV to start with.

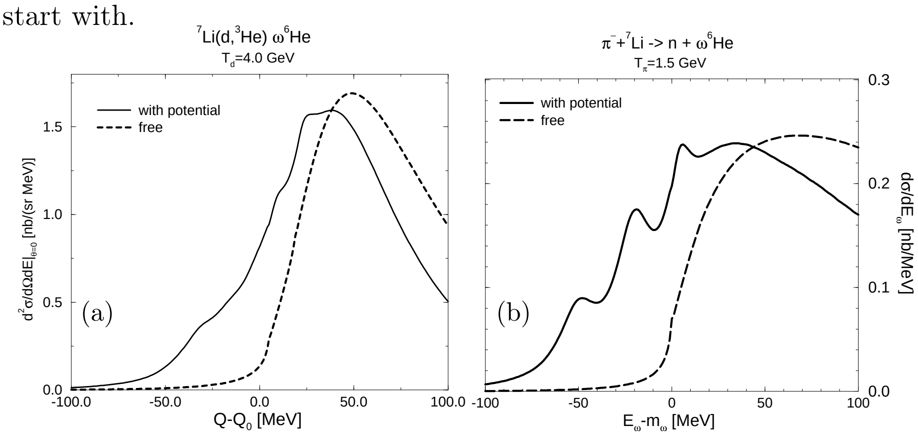

Fig. 3. Differential cross sections for the production of an ω meson using a ^{7}Li target close to threshold ($E = m_\omega$): — (a) (d,^{3}He) transfer reaction with beam kinetic energy $T_d = 4$ GeV; — (b) $\pi^- A \to n + \omega(A-1)$ reaction with a pion beam energy $T_\pi = 1.5$ GeV, assuming that the energy of the ω meson is detected through its decay into e^+e^-. Dashed curves: quasi-free production; solid curves: with inclusion of the density dependent ω meson potential (4). A flat background, not shown here, is expected to come primarily from ρ meson production.

This raises the interesting question about the possible existence of quasi-bound ω meson states in ordinary nuclei. We have solved the wave equation with the potential (4) for several nuclei up to $A = 40$ and found that such states are indeed likely to be formed. For example, the energies of deeply bound s-states turn out to be about $-50MeV$ for $A = 6$ and -90 MeV for $A = 40$. The corresponding widths of these states do not exceed 40 MeV.

Bound ω meson states could be generated in $A(d,^3\text{He})(\omega \oplus A-1)$ transfer reactions or, alternatively, using the pion-induced production process $\pi^- p \rightarrow \omega n$ in nuclei, under kinematical conditions which minimize the momentum transfer such that the ω meson is produced with small recoil momenta comparable to the nuclear Fermi momentum. Examples of calculations are shown in Figs 3(a), 3(b). These calculations use the empirical $p + d \rightarrow^3 \text{He} + \omega$ and $\pi^- p \rightarrow \omega n$ cross sections and response function techniques combined with the eikonal approach to treat distortion effects for in- and out-going particles.

The increased ω meson width in the nuclear environment prohibits the identification of isolated bound states. The differential cross sections are small, but nevertheless, a systematic downward shift of strength as compared to quasi-free ω production should be visible, even in light nuclei.

We would like to thank Volker Koch for discussions and for providing us with the CERES acceptance filter.

REFERENCES

[1] F. Klingl, N. Kaiser, W. Weise, *Z. Phys.* **A356**, 193 (1996); N. Kaiser, T. Waas, W. Weise, *Nucl. Phys.* **A 612**, 297 (1997).

[2] T. Ericson, W. Weise, *Pions and Nuclei*, Clarendon Press, Oxford 1988; T. Waas, R. Brockmann, W. Weise, *Phys. Lett.* **B 405**, 215 (1997).

[3] T. Yamazaki *et al.*, *Z. Phys.* **A355**, 219 (1996); *Phys. Lett.* **B418**, 246 (1998).

[4] G.Q. Li, C.-H. Lee, G.E. Brown, *Nucl. Phys.* **A625**, 372 (1997); W. Cassing *et al.*, *Nucl. Phys.* **A614**, 415 (1997).

[5] T. Waas, W. Weise, *Nucl. Phys.* **A625**, 287 (1997).

[6] D. Best *et al.*, (FOPI collaboration), *Nucl. Phys.* **A625**, 307 (1997); R. Barth *et al.*, (KaoS collaboration), *Phys. Rev. Lett.* **78**, 4027 (1997).

[7] F. Klingl, N. Kaiser, W. Weise, *Nucl. Phys.* **A624**, 527 (1997).

[8] F. Klingl, T. Waas, W. Weise, *Phys. Lett.* **B** (1998), to appear.

[9] T. Ullrich *et al.*, (CERES collaboration), *Nucl. Phys.* **A610**, 317c (1996).

[10] B. Friman, H.J. Pirner, *Nucl. Phys.* **A617**, 496 (1997); R. Rapp, G. Chanfray, J. Wambach, *Nucl. Phys.* **A617**, 472 (1997).

[11] G.Q. Li, C.M. Ko, G.E. Brown, *Nucl. Phys.* **A606**, 568 (1996).